

CP
HEL 9-13

AD 662178

OCEAN WAVE SIMULATION FOR ENGINEERING DESIGN

by
LEON EMMY BORGMAN

U.S. D.C.
NOV 22 1967
BC



HYDRAULIC ENGINEERING LABORATORY
COLLEGE OF ENGINEERING

UNIVERSITY OF CALIFORNIA
BERKELEY
OCTOBER, 1967

This document has been approved
for public release and sale in
distribution is unlimited.

Reproduced by the
CLEARINGHOUSE

116

University of California
Hydraulic Engineering Laboratory
Wave Research Projects

Submitted under Contract DA-49-055-CIV-ENG-64-4 with the
Coastal Engineering Research Center, Corps of Engineers, U. S. Army

Office of Research Services
Technical Report
HEL-9-13

OCEAN WAVE SIMULATION FOR ENGINEERING DESIGN

by

Leon Eary Borgman

Berkeley, California

October 1967

OCEAN WAVE SIMULATION FOR ENGINEERING DESIGN

By Leon Eury Borgman¹

INTRODUCTION

Randomly irregular waves are difficult to incorporate into engineering design. The response of the structure is usually quite complicated and often involves other factors than wave action. Thus it is frequently not possible to analytically determine the statistical characterization of the response directly from the statistical properties of the waves. In problems of this type, simulation techniques have often been the only successful method for determining solutions. These techniques have been used in a wide range of problems in physics, operations research, and other fields, wherever random factors were involved in a complicated interaction with other factors.

Basically, simulation techniques are procedures whereby artificial data having imposed statistical properties is generated by some computational means. Usually this is done in a digital computer. The artificial data is fed into the problem and the response calculated. By doing this with enough data, the equivalent of many years, or even centuries, of experience with the problem can be produced. Such factors as maximum response, or the number of times some critical value is attained, can be determined by inspection or by monitoring the output with the computer. Simulation techniques have the advantage of working for fairly complicated situations, but the disadvantage of often

¹Assoc. Prof. of Engineering Geoscience, Univ. of Calif., Berkeley, Calif.

requiring sizeable amounts of computer time.

Simulation procedures have not been used extensively in coastal engineering and ocean wave problems although several of the oil companies have used the techniques. The following study was undertaken to make the procedures more available to the engineer working with ocean wave problems and to investigate possible ways to increase the efficiency and the realism of the ocean wave and force simulations produced.

The conventions used in defining spectral density are not standardized. Differences of π and 2 show up in various papers depending on whether one-sided or two-sided spectral densities are used and whether frequencies are expressed in radians or cycles per unit time. All derivations in the following analysis will be based on the two-sided, cycles-per-unit-time spectral density relations. These will be converted to one-sided relations, where appropriate, by multiplying by 2 and taking the integration from zero to infinity instead of from minus infinity to plus infinity. The exact mathematical definitions are given in the table of notation at the back of the paper.

The sea surface elevations will be assumed to be a stationary, ergodic stochastic process produced by the addition of many infinitesimal wavelets each with a random phase. By the usual random theory of ocean waves, this leads to a Gaussian process.^{2,3}

²Pierson, W. J., Jr., "The Representation of Ocean Surface Waves by a Three-Dimensional Stationary Gaussian Process," New York University, New York, 1954.

³Kinsman, Blair, Wind Waves, Prentice-Hall Inc., Englewood Cliffs, N. J., 1965.

SIMULATION OF SEA SURFACE ELEVATIONS

Two basic methods for simulating ocean wave processes were studied. These were (a) by wave superposition and (b) by linear filters. Each method has its advantages and disadvantages. Both techniques seek to produce a mean-zero, Gaussian stochastic process which has an initially specified function as its spectral density. This initially specified function will be called the target spectral density, while the spectral density estimated from the simulated time series data will be called the realized spectral density. The target spectral density may be specified by a theoretical curve^{4,5,6} or by the discrete tabulation of a spectral density estimated from actual ocean wave recordings.

Simulation by Wave Superposition. - Let the target spectral density be denoted by $s(f)$ and suppose that F is a frequency in cycles per second such that $s(f)$ is essentially zero if f is greater than F . Let

$$0 = f_0 < f_1 < f_2 < \dots < f_N = F$$

be a partition of the interval $(0, F)$ and define

$$\Delta f_n = f_n - f_{n-1} \tag{1}$$

$$\hat{f}_n = (f_n + f_{n-1})/2 \tag{2}$$

⁴Kitaigorodskii, S. A., Application of the theory of similarity to the analysis of wind generated wave motion as a stochastic process, Izv. Akad. Nauk SSSR Ser. Geofiz., 1, 105-117; English Transl., 1, 73-80, 1962.

⁵Bretschneider, C. L., A one dimensional gravity wave spectrum: Ocean Wave Spectra, Prentice-Hall Inc., New York, 1963.

⁶Pierson, W. J., Jr. and L. Moskowitz, A proposed spectral form for fully developed wind seas based on the similarity theory of S. A. Kitaigorodskii: Jour. Geophysical Res., vol. 69, no. 24, pp. 5181-5190, 1964.

The quantity $\hat{\eta}(t)$ given by the formula

$$\hat{\eta}(t) = 2 \sum_{n=1}^N \sqrt{s(\hat{f}_n) \Delta f_n} \cos(\hat{k}_n x - 2\pi \hat{f}_n t + \bar{\Phi}_n), \quad (3)$$

where $\bar{\Phi}_n, n = 1, 2, \dots, N$, are independent random variables distributed uniformly over the interval $(0, 2\pi)$ and \hat{k}_n is defined by the relation

$$(2\pi \hat{f}_n)^2 = \hat{k}_n g \tanh \hat{k}_n d, \quad (4)$$

will approximate a Gaussian stochastic process with zero mean and spectral density $s(f)$. The symbol, d , denotes water depth and g is the acceleration due to gravity. A standard subroutine is available on most computers to generate independent uniform random numbers that may be used for $\bar{\Phi}_n$. The approximation improves as N increases and $\max_{1 \leq n \leq N} \Delta f_n$ decreases.

The simulation is based on the superposition of many waves, each having a random phase and an amplitude consistent with the energy in the target spectral density at that frequency. Fundamentally it is just the finite-difference approximation to the pseudo-integral representation for ocean waves.^{3,7,8}

$$\eta(t) = 2 \int_0^{\infty} \sqrt{s(f) df} \cos(kx - 2\pi ft + \bar{\Phi}) \quad (5)$$

One is tempted to set Δf_n equal to F/N and thus use an equal spaced subdivision of the interval $(0, F)$. However, this results in $\hat{\eta}(t)$ repeating itself exactly with period, $1/\hat{f}_1$. There are several ways to avoid the

⁷Pierson, W. J., Jr., "Wind Generated Gravity Waves," Advances in Geophysics, vol. 2, pp. 93-178, Academic Press, New York, 1955.

⁸Brown, L. J., "Methods for the Analysis of Non-Stationary Time Series with Applications to Oceanography," Hydraulic Engr. Lab. Rep. HEL 16-3, University of California, Berkeley, 1967.

periodicity. One way is to select the set of f_n values with a random number table. Another way is based on the cumulative spectrum, defined as

$$S(f) = 2 \int_0^f s(f') df' . \quad (6)$$

The quantity, $s(\hat{f}_n) \Delta f_n$, is approximately the same as $[S(f_n) - S(f_{n-1})] / 2$.

Hence (3) can be written as

$$\hat{\eta}(t) = \sqrt{2} \sum_{n=1}^N \sqrt{S(f_n) - S(f_{n-1})} \cos(\hat{k}_n x - 2\pi \hat{f}_n t + \hat{\Phi}_n) \quad (7)$$

The periodicity is avoided if the set of f_n values are chosen to make

$S(f_n) - S(f_{n-1})$ constant, say equal to a^2 , for all n values. Then (7) becomes

$$\hat{\eta}(t) = \sqrt{2} a \sum_{n=1}^N \cos(\hat{k}_n x - 2\pi \hat{f}_n t + \hat{\Phi}_n) \quad (8)$$

with f_n defined as the solution of

$$S(f_n) = (n/N) S(\infty) . \quad (9)$$

This corresponds to an equal subdivision of the energy coordinate axis for the function $S(f)$. Equation (9) is particularly easy to solve if the Bretschneider-Pierson spectral density^{5,6} is used as a theoretical model. This model has the form

$$s(f) = \frac{AB}{f^5} e^{-B/f^4} \quad (10)$$

and is directly integrable

$$S(f) = 2 \int_0^f \frac{ABe^{-B/s^4}}{s^5} ds = \frac{A}{2} \left[e^{-B/s^4} \right]_0^f = \frac{A}{2} e^{-B/f^4} \quad (11)$$

Hence $S(\infty) = A/2$ and the solution of (9) is

$$f_n = \left[\frac{B}{\log_e \left(\frac{N}{n} \right)} \right]^{1/4} \quad (12)$$

The constants A and B can be deduced from Pierson's results although it is necessary to be careful about the distinctions between one-sided and two-sided spectral densities and between radian and cycles-per-second frequencies. The above equations are based on a two-sided spectral density and cycles-per-second frequency.

The function $S(f)$ can also be computed from measured spectral densities by numerical integration and graphical determination of the f_n values. The list of f_n frequencies is then read into the simulation computer program as input data.

The simulation for sea surfaces having a directional spectral density, $s(f, \theta)$, is directly analogous to (3) and is just the discrete analogue to the psuedo integral

$$\eta(x, y, t) = 2 \int_0^{2\pi} \int_0^{\infty} \sqrt{s(f, \theta)} df d\theta \cos(kx \cos \theta + ky \sin \theta - 2\pi ft + \Phi) \quad (13)$$

That is

$$\hat{\eta}(x, y, t) = 2 \sum_{n=1}^N \sum_{m=1}^M \sqrt{s(\hat{f}_n, \hat{\theta}_m) \Delta f_n \Delta \theta_m} \cos(k_n x \cos \theta_m + k_n y \sin \theta_m - 2\pi f_n t + \Phi_{mn}) \quad (14)$$

where the interval $(0, 2\pi)$ have been subdivided

$$0 = \theta_0 < \theta_1 < \theta_2 < \dots < \theta_M = 2\pi$$

and

$$\Delta \theta_m = \theta_m - \theta_{m-1} \quad (15)$$

$$\hat{\theta}_m = (\theta_m + \theta_{m-1})/2 \quad (16)$$

Equation (14) may be computed for more than one space location using the same uniform $(0, 2\pi)$ independent random numbers for each computation. If N and M are large enough, the simulated values of $\hat{\eta}(x_k, y_k, t)$, $k = 1, 2, 3, \dots$, will

maintain approximately the correct intercorrelations and cross-spectral densities.

Simulation by Linear Filtering. - Let x_1, x_2, x_3, \dots , be any initial sequence of numbers and let $a_{-N}, a_{-N+1}, a_{-N+2}, \dots, a_{N-1}, a_N$ be any fixed sequence of constants. Then the sequence obtained by

$$y_k = \sum_{n=-N}^N a_n x_{k-n} \quad k = N+1, N+2, N+3, \dots \quad (17)$$

is called the output obtained by applying the digital filter

$\{a_n, n = 0, \pm 1, \pm 2, \dots, \pm N\}$ to the initial sequence $\{x_n, n = 1, 2, \dots\}$.

The basic problem (the design of the digital filter) is the determination of the values of a_n which yield y_n having particular desired properties. The procedure for designing a digital filter is easy to follow if certain basic relations from Fourier transform theory are kept in mind.

Fundamental Fourier Relations. - A linear integral operator with kernel, $k(\tau)$, acting on the input, $x(t)$, to produce an output, $y(t)$, may be written

$$y(t) = \int_{-\infty}^{\infty} k(\tau)x(t-\tau)d\tau . \quad (18)$$

The input and output will be assumed real; hence, the kernel function is also real. The Fourier transform of the kernel,

$$K(f) = \int_{-\infty}^{\infty} e^{-i2\pi f\tau} k(\tau)d\tau , \quad (19)$$

is called the system function of the linear operator. By Euler's relation,

$$e^{-i\theta} = \cos \theta - i \sin \theta , \quad (20)$$

so $K(f)$ can be also written in terms of trigonometric functions as

$$K(f) = \int_{-\infty}^{\infty} k(\tau) \cos 2\pi f\tau d\tau - i \int_{-\infty}^{\infty} k(\tau) \sin 2\pi f\tau d\tau \quad (21)$$

Relative to the variable, f , the real part of $K(f)$ is, thus, symmetric about $f = 0$, and the imaginary part of $K(f)$ is skew symmetric. That is

$$\Re [K(f)] = \Re [K(-f)] \quad (22)$$

$$\Im [K(f)] = - \Im [K(-f)] \quad (23)$$

The two basic spectral density interrelationships between $x(t)$ and the $y(t)$ given by (18) are ⁹

$$s_{yy}(f) = |K(f)|^2 s_{xx}(f) \quad (24)$$

$$s_{xy}(f) = K(f) s_{xx}(f) \quad (25)$$

A further relation is that $y(t)$ will have mean zero and be normally distributed if $x(t)$ has these same properties.

The digital filter may be written as a linear integral operator if Dirac delta functions are introduced. Suppose that y_k and x_n are related to $y(t)$ and $x(t)$ by the following equivalence.

$$y_k = y(k \Delta t) \quad , \quad k = 0, 1, 2, 3, \dots \quad (26)$$

$$x_n = x(n \Delta t) \quad , \quad n = 0, 1, 2, 3, \dots \quad (27)$$

Then the digital filter in (17) may be rewritten

$$\begin{aligned} y(t) &= \sum_{n=-N}^N a_n x(t - n \Delta t) \\ &= \int_{-\infty}^{\infty} \left[\sum_{n=-N}^N a_n \delta(\tau - n \Delta t) \right] x(t - \tau) d\tau \quad , \quad \text{for } t = 0, \Delta t, 2\Delta t, \dots \end{aligned} \quad (28)$$

⁹ Bendat, J. S. and Piersol, A. G., Measurement and Analysis of Random Data, John Wiley, New York, 1966, pp. 98-99, eqs. (3.137) and (3.138).

Thus the kernel of the digital filter, which will be denoted by $\hat{k}(\tau)$, is

$$\hat{k}(\tau) = \sum_{n=-N}^N a_n \delta(\tau - n\Delta t) \quad (29)$$

and the system function (derived in appendix I) is

$$\begin{aligned} \hat{K}(f) &= \int_{-\infty}^{\infty} e^{-i2\pi f\tau} \hat{k}(\tau) d\tau \\ &= A_0 + 2 \sum_{n=-N}^N A_n \cos(n\pi f/F) - i 2 \sum_{n=-N}^N B_n \sin(n\pi f/F) \end{aligned} \quad (30)$$

where

$$A_n = 1/2 [a_n + a_{-n}] \quad (31)$$

$$B_n = 1/2 [a_n - a_{-n}] \quad (32)$$

$$F = 1/2 \Delta t \quad (33)$$

Equation (30) is the key to the design of a digital filter to approximate an arbitrary linear integral operator having a real kernel. Basically one has only to make $\hat{K}(f)$ have the same shape as the system function $K(f)$ for the arbitrary operator. That is, the A_n and B_n need to be determined so that

$$\mathcal{R}[K(f)] \approx A_0 + 2 \sum_{n=1}^N A_n \cos(n\pi f/F) \quad (34)$$

$$\mathcal{I}[K(f)] \approx 2 \sum_{n=1}^N B_n \sin(n\pi f/F) \quad (35)$$

The right hand side of these equations have period $2F$. If N is large enough,

the approximation can be made quite good between $-F$ and $+F$, but outside that interval $\hat{K}(f)$ will be repeated with period $2F$. However, if F is large enough so that the response of the filter to frequencies greater than F is of no importance in the intended application, then the periodicity of $\hat{K}(f)$ will cause no difficulty. Since $F = 1/2 \Delta t$, making F large is equivalent to moving the digital filter along a sequence with tighter spacing on the time axis.

The constants A_n and B_n may be determined by the usual procedures for fitting a Fourier series

$$A_n = \frac{1}{F} \int_0^F \mathcal{R} [K(f)] \cos (n\pi f/F) df \quad (36)$$

$$B_n = \frac{1}{F} \int_0^F \mathcal{I} [K(f)] \sin (n\pi f/F) df \quad (37)$$

(Standard subroutines are available at most digital computer installations to make these computations quickly and easily. The new fast Fourier methods are particularly appropriate here ¹⁰.)

Once the A_n and B_n are computed, the coefficients a_n follow immediately from (31) and (32)

$$\begin{aligned} a_0 &= A_0 \\ a_n &= A_n + B_n \\ a_{-n} &= A_n - B_n \end{aligned} \quad \text{for } n = 1, 2, 3, \dots, N \quad (38)$$

¹⁰Cooley, J. W., and Tukey, J. W., "An Algorithm for the Machine Calculation of Complex Fourier Series," Jour. of Math. of Computations, April, 1965, pp. 297-301.

Simulating $\eta(t)$ at One Space Location. - The random input, $x(t)$, is called white noise if the spectral density of $x(t)$ is unity. White noise may be approximated by a sequence of independent normally distributed random variables x_1, x_2, x_3, \dots , each of which has mean zero and unit variance. Since subroutines for generating independent normal random variables are available for most computers, white noise is a convenient input for simulation by a linear integral operator (18) or its digital approximator, (17).

Suppose it is desired to produce a simulated sea surface elevation, $\eta(t)$, which has spectral density, $s(f)$. This can be produced from (18) with white noise input if

$$K(f) = \sqrt{s(f)} \quad . \quad (39)$$

For if $\eta(t)$ is formally identified with the $y(t)$ produced by (18), then (24) gives

$$s_{\eta\eta}(f) = |K(f)|^2 s_{xx}(f) = s(f) \quad (40)$$

It remains only to determine the digital filter constants, a_n , so that the digital filter system function $\hat{K}(f)$ closely approximates $K(f) = \sqrt{s(f)}$. This is achieved by the Fourier series fitting procedure indicated by (34) to (37). Since $\sqrt{s(f)}$ has no imaginary part, only A_0, A_1, \dots, A_n need to be determined. The cutoff frequency, F , may be any convenient value such that $s(f)$ is essentially zero for higher frequencies. However computations are simplified if F corresponds to a Δt interval which is an exact fraction or multiple of the time scale unit.

The introduction of a directional spectral density, $s(f, \theta)$, as the target produces no real complications if one is interested only in one space location. All that is necessary is to integrate out θ . That is,

$$s(f) = \int_0^{2\pi} s(f, \theta) d\theta \quad (41)$$

and then proceed as in (39) and following.

Simulating Several Simultaneous Time Series. - The basic difficulty with simultaneous simulation, is that the individual simulations have to produce the intercorrelations or interspectral densities between the various series which have been previously specified. One procedure which maintains these interrelationships is as follows.

Suppose M time series are to be simulated. These will be denoted by $y_1(t), y_2(t), \dots, y_M(t)$. The simulations will be developed from M independent inputs, $x_1(t), x_2(t), \dots, x_M(t)$. The idealized simulation for the m-th time series will be given by

$$y_m(t) = \sum_{j=1}^m \int_{-\infty}^{\infty} k_{mj}(\tau) x_j(t - \tau) d\tau, \text{ for } m = 1, 2, \dots, M \quad (42)$$

(The integral operators will be replaced by digital filter approximations in the actual computations.)

Let $s_{mr}(f)$ represent the cross spectral density between $y_m(t)$ and $y_r(t)$. The kernels $k_{mj}(\tau)$, or the corresponding system functions $K_{mj}(f)$, can be selected to produce the required cross spectral densities. The key relationship utilized in the determination of the $K_{mj}(f)$ is (see appendix II)

$$s_{mr}(f) = \sum_{j=1}^r K_{mj}(f) \overline{K_{rj}(f)} s_{x_j x_j}(f), \quad \begin{matrix} r = 1, 2, \dots, m \\ m = 1, 2, \dots, M \end{matrix} \quad (43)$$

where it is assumed that $m \geq r$. (Note $\overline{s_{rm}(f)} = s_{mr}(f)$). The over bar in the previous equations indicates complex conjugation. If (43) is expanded into

a system of equations, with independent white noise inputs, it becomes

$$\begin{aligned}
 s_{11}(f) &= |K_{11}(f)|^2 \\
 s_{21}(f) &= K_{21}(f) \overline{K_{11}(f)} \\
 s_{22}(f) &= |K_{21}(f)|^2 + |K_{22}(f)|^2 \\
 s_{31}(f) &= K_{31}(f) \overline{K_{11}(f)} \\
 s_{32}(f) &= K_{31}(f) \overline{K_{21}(f)} + K_{32}(f) \overline{K_{22}(f)} \\
 s_{33}(f) &= |K_{31}(f)|^2 + |K_{32}(f)|^2 + |K_{33}(f)|^2 \\
 &\text{etc.}
 \end{aligned}
 \tag{44}$$

This system of equations can be solved sequentially

$$\begin{aligned}
 K_{11}(f) &= \sqrt{s_{11}(f)} \\
 K_{21}(f) &= s_{21}(f) / \sqrt{s_{11}(f)} \\
 K_{22}(f) &= \left[s_{22}(f) - |K_{21}(f)|^2 \right]^{1/2} \\
 K_{31}(f) &= s_{31}(f) / \sqrt{s_{11}(f)} \\
 K_{32}(f) &= \left[s_{32}(f) - K_{31}(f) \overline{K_{21}(f)} \right] / K_{22}(f) \\
 K_{33}(f) &= \left[s_{33}(f) - |K_{31}(f)|^2 - |K_{32}(f)|^2 \right]^{1/2} \\
 &\text{etc.}
 \end{aligned}
 \tag{45}$$

The design of the simulation equation is completed now by determining $\hat{K}_{mj}(f)$ as in (30), (34) and (35) to fit $K_{mj}(f)$ as determined by (46). This in turn determines the digital filter coefficients, a_{nmj} , needed to approximate the kernel associated with the system function $K_{mj}(f)$. Then the final simulation equation reduces to

$$y_m(k \Delta t) = \sum_{j=1}^m \sum_{n=-N}^N a_{nmj} x_{j,k-n} \quad , \quad m = 1, 2, \dots, M \quad (46)$$

where $x_{j,n}$ for $n = 1, 2, 3, 4, \dots$ is the j -th generated sequence of independent, mean zero, unit variance, normal random variables.

If the input $x_j(t)$ is not white noise the system of equations represented by (43) can still be solved sequentially with only slight additional complications.

Simulating Several Sea Surface Elevations. - Let $\eta_1(t), \eta_2(t), \dots, \eta_M(t)$ represent the sea surface elevations at time t at M space locations. If $y_m(t)$ is replaced with $\eta_m(t)$ in the development in the previous section, then (46) gives the required digital filter. The spectral densities $s_{11}(f), s_{22}(f), s_{33}(f), \dots$, are all set equal to the target spectral density, $s(f)$, for the sea surface elevations, which is the same for all locations. The cross-spectral densities have a slightly different formulation depending on whether the sea surface spectrum is unidirectional (say directed along the x -axis) or directional. In the first case, suppose the m locations are x_1, x_2, \dots, x_M . The cross-spectral density between $\eta(x_m, t)$ and $\eta(x_r, t)$ is¹¹

¹¹Brown, L. J., and Borgman, L. E., "Tables of the Statistical Distribution of Ocean Wave Forces and Methods for the Estimation of C_D and C_M ," Wave Research Report HRL 9-7, Hydraulic Engineering Laboratory, University of California, Berkeley, Calif., 1966, Appendix C.

$$s_{mr}(f) = s(f) \left[\cos k(x_r - x_m) - i \sin k(x_r - x_m) \right] \quad (47)$$

In the second case, let $s(f, \theta)$ be the directional spectral density for the sea surface elevations and $(x_1, y_1), (x_2, y_2), (x_3, y_3), \dots, (x_M, y_M)$ be the M space locations. Then

$$s(f) = \int_0^{2\pi} s(f, \theta) d\theta \quad (48)$$

$$s_{mr}(f) = \int_0^{2\pi} s(f, \theta) \cos \{k(x_r - x_m) \cos \theta + k(y_r - y_m) \sin \theta\} d\theta \\ - i \int_0^{2\pi} s(f, \theta) \sin \{k(x_r - x_m) \cos \theta + k(y_r - y_m) \sin \theta\} d\theta \quad (49)$$

Distortions of $\hat{\eta}(t)$ to Produce Skewness. - Steep waves in nature have skewed surface elevations. That is, the crests tend to be higher above mean sea level than the troughs are below. The simulation procedures previously given produce Gaussian or normally-distributed sea surface elevations which are not skewed. Obviously high wave conditions violate a number of assumptions in the statistical theory of waves, most importantly perhaps the assumed linear superposition. However, until a successful statistical theory of waves of finite height is developed, the engineer is faced with doing as well as he can with the existing theory.

The present simulations can be made to appear a little more like the real sea if skewness is introduced. One way this can be done is as follows. The Gaussian sea surface simulation, $\hat{\eta}(t)$, is developed as before. Then a normal to gamma transformation¹² which maintains a zero mean and introduces the required

¹²Campbell, G. A., "Probability Curves Showing Poisson's Exponential Summation," Bell System Technical Journal, vol. 2, 1923, pp. 95-113.

skewness, s_k ,

$$\begin{aligned}
 Q_1 &= (\hat{\eta}^2 - 1)/3 \\
 Q_2 &= (\hat{\eta}^3 - 7\hat{\eta})/36 \\
 Q_3 &= (-3\hat{\eta}^4 - 7\hat{\eta}^2 + 16)/810 \\
 Q_4 &= (9\hat{\eta}^5 + 256\hat{\eta}^3 - 433\hat{\eta})/38880 \\
 Q_5 &= (12\hat{\eta}^6 - 243\hat{\eta}^4 - 923\hat{\eta}^2 + 1472)/204120 \\
 Q_6 &= (-3753\hat{\eta}^7 - 4353\hat{\eta}^5 + 289517\hat{\eta}^3 + 289717\hat{\eta})/146966400 \\
 \hat{\eta}_s(t) &= \hat{\eta} + \sum_{n=1}^6 Q_n (s_k/2)^n
 \end{aligned} \tag{50}$$

is made to introduce more peaked crests and flatter troughs. Skewness may be introduced in other ways. The above is just one convenient and thoroughly investigated procedure. The whole topic deserves considerable further research.

How much skewness should be introduced? If an extensive piece of actual wave record is available for the sea surface elevations that are to be simulated, one scheme of calculation would be: (a) Compute the skewness for the wave record

$$s_k = \frac{\frac{1}{R} \int_0^R \eta^3(t) dt}{\left[\frac{1}{R} \int_0^R \eta^2(t) dt \right]^{3/2}} \tag{51}$$

(where R is the length of record). (b) Make the gamma-to-normal transformation¹³ which produces an unskewed version of the wave record with the same zero mean

¹³Riordan, John, "Inversion Formulas in Normal Variable Mapping," Annals of Mathematical Statistics, vol. 20, 1949, pp. 417-425.

$$\begin{aligned}
x_1 &= (-\eta_s^2 + 1) / 3 \\
x_2 &= (7\eta_s^3 - \eta_s) / 36 \\
x_3 &= (-219\eta_s^4 + 14\eta_s^2 + 13) / 1620 \\
x_4 &= (3993\eta_s^5 - 152\eta_s^3 + 119\eta_s) / 38880 \\
x_5 &= (-67227\eta_s^6 + 1707\eta_s^4 - 2041\eta_s^2 - 3095) / 816480 \\
x_6 &= (10059417\eta_s^7 - 179223\eta_s^5 + 271427\eta_s^3 + 215827\eta_s) / 146966400 \\
\eta(t) &= \eta_s + \sum_{n=1}^6 x_n (s_k/2)^n
\end{aligned} \tag{52}$$

This system of equations gives two more terms than were contained in Riordan's paper and also corrects a misprint in the x_4 formula. Both (50) and (52) can be truncated to fewer terms if the accuracy requirements permit. (c) Compute the spectral density on the unskewed version and make a normal simulation, $\hat{\eta}(t)$. (d) Re-introduce the skewness calculated in (51) by making the normal-to-gamma transformation given by (50).

The above scheme needs to be evaluated against actual experience. It represents only one possible procedure. Undoubtedly further study will suggest others. Perhaps the mode of the spectral density, the rms wave amplitude, and the water depth could be used to get η_c/H from existing graphs.¹⁴ This, in turn, might provide an estimate of the skewness that needs to be introduced.

¹⁴Lean, R. G., "Stream Function Wave Theory; Validity and Application," Coastal Engineering Santa Barbara Specialty Conference, ASCE, October, 1965, p. 282.

SIMULATION OF VELOCITIES AND ACCELERATIONS

The horizontal components of the water velocity and acceleration at some fixed elevation above the sea floor can be simulated with filters using either white noise or the sea surface elevations as basic input. A unidirectional spectrum and a white noise input requires the same procedures previously developed except that the spectral densities for the horizontal velocity and acceleration need to be introduced.

$$s_{vv}(f) = (2\pi f)^2 \frac{\cosh^2 kz}{\sinh^2 kd} s_{\eta\eta}(f) \quad (53)$$

$$s_{aa}(f) = (2\pi f)^4 \frac{\cosh^2 kz}{\sinh^2 kd} s_{\eta\eta}(f) \quad (54)$$

The cross-spectral density between the horizontal velocity and acceleration is zero. Hence the two digital filters can be designed separately and applied to two independent white noise inputs.

The situation for a directional spectral density is considerably more complicated. For one thing, there are two horizontal components for both the velocity and the acceleration. The cross-spectral densities between these components are not all zero. Thus the procedure for simultaneous simulations of time series needs to be introduced (see (42) and (43)). The required cross-spectral densities are listed by Wave Research Report 9-12.^{15a}

The generation of velocities and accelerations using the sea surface elevation as input is based on (25) and the cross-spectral densities of velocity

^{15a} Borgman, L. E., "Tables of Ocean Wave Cross-Spectral Formulas," Wave Research Report HEL 9-12, Hydraulic Engineering Laboratory, University of California, Berkeley, Calif., 1967.

and acceleration with $\eta(t)$. The required spectral densities^{15a} are, for the unidirectional spectrum

$$s_{\eta(x,t), v(x+h,t)}(f) = \left[(2\pi f) \frac{\cosh kz}{\sinh kd} (\cos kh - i \sin kh) \right] s_{\eta\eta}(f) \quad (55)$$

$$s_{\eta(x,t), a(x+h,t)}(f) = \left[(2\pi f)^2 \frac{\cosh kz}{\sinh kd} (\sin kh + i \cos kh) \right] s_{\eta\eta}(f) \quad (56)$$

Hence by (25)

$$K_v(f; z) = (2\pi f) \frac{\cosh kz}{\sinh kd} (\cos kh - i \sin kh) \quad (57)$$

$$K_a(f; z) = (2\pi f)^2 \frac{\cosh kz}{\sinh kd} (\sin kh - i \cos kh) \quad (58)$$

Thus for a unidirectional spectral density, the system functions $K_v(f; z)$ and $K_a(f; z)$ do not depend on the particular sea surface spectral density that is to be used. The digital filters can be determined by (34) and (35) without references to $s_{\eta\eta}(f)$. This yields an estimator equation that may be written

$$\hat{v}(k \Delta t) = \sum_{n=-N}^N a_{vn} \eta(k \Delta t - n \Delta t) \quad (59)$$

$$\hat{a}(k \Delta t) = \sum_{n=-N}^N a_{an} \eta(k \Delta t - n \Delta t) \quad (60)$$

Somewhat similar procedures were used by Reid in a study of wave forces^{15b}.

The corresponding procedure for a directional spectral density is analogous. The cross-spectral densities may be obtained from Tech Report HEL 9-12.^{15a} The system functions intrinsically depend on the directional spectral density for the sea surface.

Both the unidirectional and the directional spectral density cases can be

^{15b}Reid, R. O., "Correlation of Water Level Variations with Wave Forces on a Vertical Pile for Nonperiodic Waves, Proc. Sixth Conf. on Coastal Eng., pp. 749-786, The Engineering Foundation, Univ. of Calif., 1958.

handled fairly directly with the procedure for simulation by wave superposition. The linear wave theory formula for the quantity to be simulated is written down using as wave amplitude, $\sqrt{4s(\hat{f}_n) \Delta f_n}$ in the unidirectional case, and $\sqrt{4s(\hat{f}_n, \hat{\theta}_m) \Delta f_n \Delta \theta_m}$ in the directional case. For both cases a random phase is inserted. In the directional case, kx in the linear wave theory is replaced with $kx \cos \theta + ky \sin \theta$ and the whole term is multiplied by $\cos \theta$ for the x component and $\sin \theta$ for the y component. Then the expression is summed over all \hat{f}_n (and $\hat{\theta}_m$ in the 2-D situation). Examples of this procedure are

linear theory:

$$v_x = a(2\pi f) \frac{\cosh kz}{\sinh kd} \cos(kx - 2\pi ft) \quad (61)$$

simulation for unidirectional spectrum:

$$\hat{v}_x(t) = \sum_{n=1}^N \sqrt{4s(\hat{f}_n) \Delta f_n} (2\pi \hat{f}_n) \frac{\cosh \hat{k}_n z}{\sinh \hat{k}_n d} \cos(\hat{k}_n x - 2\pi \hat{f}_n t + \Phi_n) \quad (62)$$

simulation for directional spectrum: $\hat{v}_x(t) =$

$$= \sum_{n=1}^N \sum_{m=1}^M \sqrt{4s(\hat{f}_n, \hat{\theta}_m) \Delta f_n \Delta \theta_m} (2\pi \hat{f}_n) \frac{\cosh \hat{k}_n z}{\sinh \hat{k}_n d} \cos \hat{\theta}_m \cos(\hat{k}_n x \cos \hat{\theta}_m + \hat{k}_n y \sin \hat{\theta}_m - 2\pi \hat{f}_n t + \Phi_{mn}) \quad (63)$$

The simulation by wave superposition has the one grave disadvantage of being time consuming. However this is balanced by the fact that simultaneous simulations of several quantities automatically maintain the proper intercorrelation.

SIMULATION OF WAVE FORCES

The usual formula for wave forces on a one-foot section of vertical piling

$$\phi = C_D \frac{w}{2g} Dv|v| + C_M \frac{w}{g} \frac{\pi D^2}{4} a \quad (64)$$

can be applied to the velocity and acceleration simulations developed in the previous section to give force simulations. This procedure could be followed to simulate the total force on a structure composed of vertical cylinders. Simulations could be made for the forces at a series of locations down each pile, and the forces could be numerically integrated to give total force.

Modifications to Give Better Agreement with Nature. - The statistical theory for waves is based on linear wave theory. But linear waves have infinitesimal amplitudes which do not extend measurably above still water level. How does one then compute velocities and accelerations for elevations above this level? To what elevation up the pile does the integration proceed if it is not carried just to still water level? If the velocities and accelerations are simulated from the sea surface elevations at the pile, the second question is answered immediately. The integration is carried to the sea surface. The first question, however, can only be answered with approximations. A conservative approximation for velocities and accelerations above mean sea level is to use the same formulas that hold below sea level. The forces are computed for $z > d$ and ignored if $\eta(t) < z$. An alternative approximation is to "stretch" the still water level in the formula up to the sea surface. In this procedure, the force is simulated at a series of elevations between the sea floor and still water level. The force at elevation z is assumed to act actually at elevation $z[d + \eta(t)]/d$. That is the force displaced upward or downward depending on whether $\eta(t)$ is positive or negative. This procedure has the advantage that the integration for total force can be carried to $z = d$ in terms of the force simulation and the total force then "stretched"

to correct for $\eta(t)$.

It is difficult to evaluate the accuracy of these approximations. They both obviously fail if the waves get very high. Yet they, at least, provide one approach to the problem. The ultimate answer is, of course, a statistical theory for waves of finite height. Until that is available, irregular waves of non-permanent form having a statistical nature can only be treated with a "patched-up" linear statistical theory.

The force simulation with (64) being applied to (59) and (60) and then numerically integrated has one grave disadvantage in computer computations. It is time consuming. An approximate procedure which is faster would be better. After all, (64) is known to be only an imperfect approximation of the actual force.¹⁶ So some degree of further approximation is not particularly objectionable.

Approximations to the Force Formula. - A faster simulation would result if the total force on a vertical pile could be expressed as a single operator acting on the sea surface elevations or, alternatively, acting on white noise. The inertial force, the second term on the right hand side of (64), can be so expressed. If $a(t;z)$ is the acceleration at elevation z on the pile at time t and $k_a(\tau;z)$ is the kernel for $a(t;z)$ then

$$a(t;z) = \int_{-\infty}^{\infty} k_a(\tau;z) \eta(t - \tau) d\tau \quad (65)$$

¹⁶Wiegel, R. L., Beebe, K. E., and Moon, James, "Ocean Wave Forces on Circular Cylindrical Piles." Journal of the Hydraulics Division, ASCE, vol. 83, no. HY2, Proc. Paper 1199, April, 1957.

The total inertial force becomes then

$$\begin{aligned} \text{total inertial force} &= [(\eta(t)+d)/d] \int_0^d C_M \frac{w}{g} \frac{\pi D^2}{4} \int_{-\infty}^{\infty} k_a(\tau; z) \eta(t-\tau) d\tau dz \\ &= [(\eta(t)+d)/d] \int_{-\infty}^{\infty} \left[C_M \frac{w}{g} \frac{\pi D^2}{4} \int_0^d k_a(\tau; z) dz \right] \eta(t-\tau) d\tau \end{aligned} \quad (66)$$

This eliminates the vertical integration. The quantity in the bracket is the new total kernel that must be approximated with a digital filter. The "stretching" correction for forces above still water level has been introduced into the equation.

The drag force, the first term on the right side of (64), does not simplify this way. If

$$v(t; z) = \int_{-\infty}^{\infty} k_v(\tau; z) \eta(t - \tau) d\tau \quad (67)$$

is substituted into the expression for drag force, one gets for the total drag force on a vertical pile

$$\left[(\eta(t)+d)/d \right] \int_0^d C_D \frac{w}{2g} D \int_{-\infty}^{\infty} k_v(\tau; z) \eta(t-\tau) d\tau \left| \int_{-\infty}^{\infty} k_v(\tau; z) \eta(t-\tau) d\tau \right| dz \quad (68)$$

The absolute value interferes with the shuffling of integrals which simplified (66).

In an earlier paper,¹⁷ the term $v|v|$ in the drag force formula was found to be approximated very nicely, at least relative to predicting the force spectral

¹⁷ Borgman, L. E., "Spectral Analysis of Ocean Wave Forces on Piling," Journal of Waterways and Harbors Division, ASCE, vol. 93, no. WW2, Proc. Paper 5247, May 1967, pp. 129-156. (See p.151, eq.(74)).

density, by

$$v|v| \approx v_{\text{rms}} \sqrt{(8/\pi)} v \quad (69)$$

Here, v_{rms} is the standard deviation, or root-mean-square value for the velocity. In essence $|v|$ has been replaced by $v_{\text{rms}} \sqrt{(8/\pi)}$. The effect of the approximation is easier to comprehend if the linear theory versions are introduced. From the usual formulas for velocity

$$v|v| = \left[\frac{\pi H}{T} \frac{\cosh kz}{\sinh kd} \right]^2 \cos \theta |\cos \theta| \quad (70)$$

$$v_{\text{rms}} \sqrt{\frac{8}{\pi}} v = \left[\frac{\pi H}{T} \frac{\cosh kz}{\sinh kd} \right]^2 \sqrt{\frac{8}{2\pi}} \cos \theta \quad (71)$$

Since $\sqrt{8/2\pi}$ is not too much larger than unity, the approximation replaces $v|v|$ with a cosine oscillation whose maximum amplitude (at $\theta = 0$) is only slightly greater than $v|v|$. Both expressions are zero at $\theta = \pi/2$.

The analytic basis for (69) becomes clear if one asks for the most accurate linear estimate of $v|v|$, assuming v is normally distributed with mean zero and standard deviation $\sigma = v_{\text{rms}}$. That is, what is the constant c which minimizes

$$Q = \int_{-\infty}^{\infty} [v|v| - cv]^2 \frac{e^{-v^2/2\sigma^2}}{\sqrt{2\pi}\sigma} dv \quad (72)$$

By calculus, Q has an extremum if

$$0 = \frac{\partial Q}{\partial c} = -2 \left[\int_{-\infty}^{\infty} v^2 |v| \frac{e^{-v^2/2\sigma^2}}{\sqrt{2\pi}\sigma} dv - c \int_{-\infty}^{\infty} v^2 \frac{e^{-v^2/2\sigma^2}}{\sqrt{2\pi}\sigma} dv \right] \quad (73)$$

or

$$c = \frac{\int_{-\infty}^{\infty} v^2 |v| \frac{e^{-v^2/2\sigma^2}}{\sqrt{2\pi}\sigma} dv}{\sigma^2} = \sigma \sqrt{(8/\pi)} \quad (74)$$

Further analysis shows that this value minimizes Q . The result agrees exactly with (69), hence cv is the best linear estimator for $v|v|$ in the least-square sense. The procedure can be extended to the cubic and quintic approximations. There, one seeks the values of the constants which minimize

$$Q_3 = \int_{-\infty}^{\infty} [v|v| - c_1v - c_3v^3]^2 \frac{e^{-v^2/2\sigma^2}}{\sqrt{2\pi}\sigma} dv \quad (75)$$

or

$$Q_5 = \int_{-\infty}^{\infty} [v|v| - c_1v - c_3v^3 - c_5v^5]^2 \frac{e^{-v^2/2\sigma^2}}{\sqrt{2\pi}\sigma} dv \quad (76)$$

The solutions which minimize (75) and (76) are determined by differentiation with respect to the unknown constants to be

$$c_1v + c_3v^3 = v_{rms} \sqrt{(2/\pi)} v + \sqrt{(2/9\pi)} (v^3/v_{rms}) \quad (77)$$

and

$$c_1v + c_3v^3 + c_5v^5 = \sqrt{(2/\pi)} [(3v_{rms}/4) v + (1/2 v_{rms}) v^3 - (1/60 v_{rms}^3) v^5] \quad (78)$$

A comparison of the linear, cubic, and quintic approximations with $v|v|$ is shown in Fig. 1. The approximations have been made dimensionless by changing to the variable

$$x = (v/v_{rms}) \quad (79)$$

Then the three approximations become in terms of x

$$(v|v|/v_{rms}^2) = x|x| \approx \sqrt{(8/\pi)} x \quad (80)$$

$$\approx \sqrt{(2/\pi)} [x + (1/3) x^3] \quad (81)$$

$$\approx \sqrt{(2/\pi)} [(3/4)x + (1/2)x^3 - (1/60)x^5] \quad (82)$$

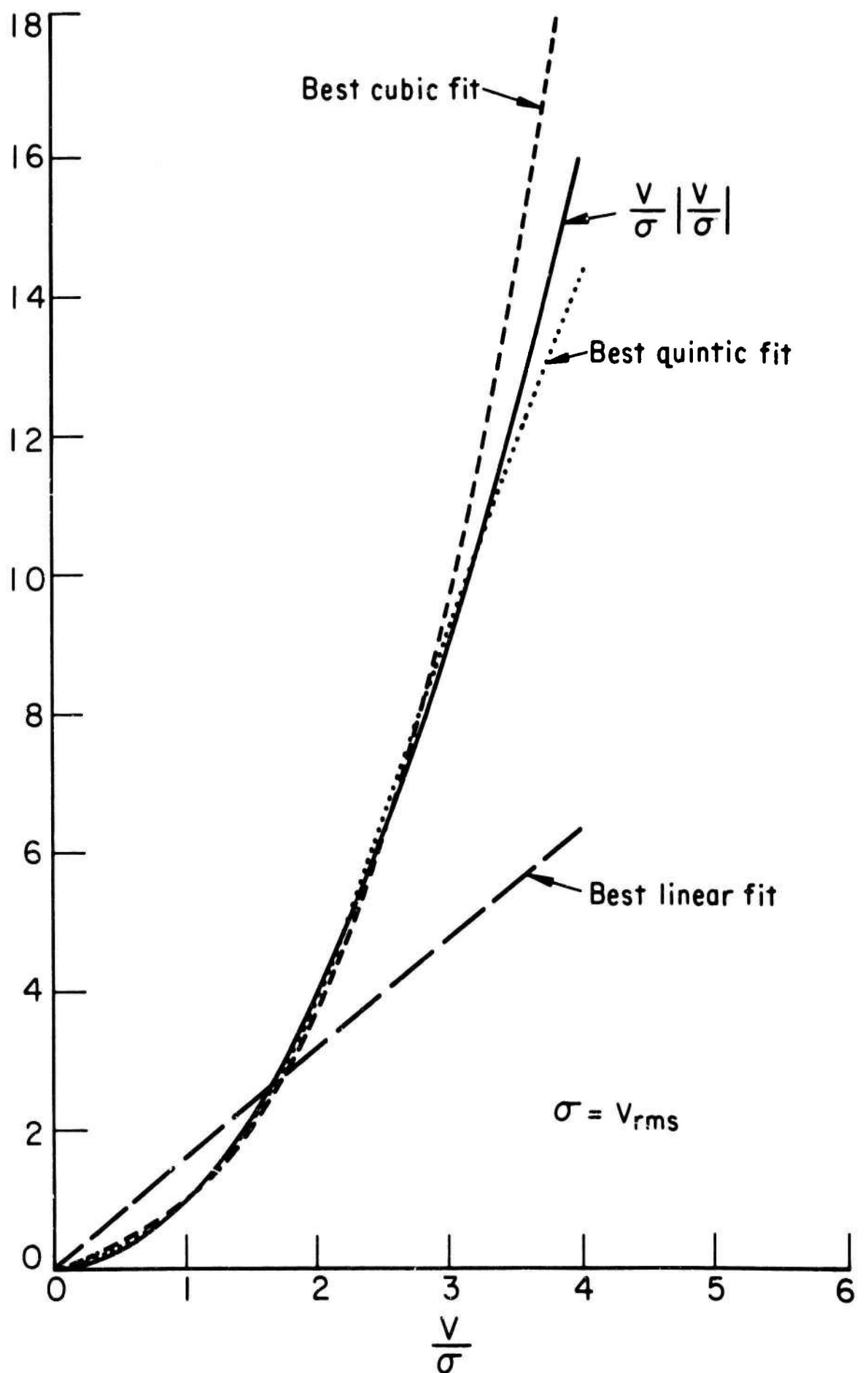


Fig. 1. Polynomial approximation to $v|v|$.

An examination of Fig. 1 shows that the linear approximation does a fair job for $|x| < 2$; that is, if the velocity is within plus or minus two standard deviations. Since according to normal theory this happens 95% of the time, it is entirely reasonable that the linear approximation would do a good job on estimating a curve like the spectral density which depends on the average behavior of the velocity values.

The cubic approximation is quite accurate out to more than three standard deviations and the quintic is good to almost four standard deviations. The quintic approximation is only slightly better than the cubic. The cubic approximation, however, is quite an improvement over the linear expression.

All of the above approximations were derived under the assumption that the mean value of v was zero (i.e., there was no steady current present). The same analysis can be carried through if the mean of v is not necessarily zero, although the mathematics is more complicated. Even powers of v must be included and the normal density has to include the parameter for the mean. As an example, the least-square linear estimate for a normal v with mean m and variance σ^2 is determined by minimizing

$$Q = \int_{-\infty}^{\infty} [v|v| - c_0 - c_1 v] \frac{e^{-(v-m)^2/2\sigma^2}}{\sqrt{2\pi}\sigma} dv \quad (83)$$

Let

$$\phi(x) = \frac{e^{-x^2/2}}{\sqrt{2\pi}} \quad (84)$$

$$\Phi(x) = \int_{-\infty}^x \frac{e^{-t^2/2}}{\sqrt{2\pi}} dt \quad (85)$$

The least square solution for (83) is

$$c_0 + c_1 v = (\sigma^2 - m^2) \left[2\Phi\left(\frac{m}{\sigma}\right) - 1 \right] - 2 m \sigma \phi\left(\frac{m}{\sigma}\right) + \\ + \left\{ 2m \left[2\Phi\left(\frac{m}{\sigma}\right) - 1 \right] - 4 \sigma \phi\left(\frac{m}{\sigma}\right) \right\} v \quad (86)$$

Total Force on a Single Vertical Pile. - The filter concept in (18) can be extended to higher orders

$$y(t) = \int_{-\infty}^{\infty} k_1(\tau) x(t-\tau) d\tau + \int_{-\infty}^{\infty} \int_{-\infty}^{\infty} k_2(\tau_1, \tau_2) x(t-\tau_1) x(t-\tau_2) d\tau_1 d\tau_2 \\ + \int_{-\infty}^{\infty} \int_{-\infty}^{\infty} \int_{-\infty}^{\infty} k_3(\tau_1, \tau_2, \tau_3) x(t-\tau_1) x(t-\tau_2) x(t-\tau_3) d\tau_1 d\tau_2 d\tau_3 \\ + \dots \quad (87)$$

A second-order filter would consist of the first two terms, a third-order filter of the first three terms, etc. If the first-order approximation to the drag force is used, the difficulty in (68) is avoided completely. The total drag force becomes (approximately)

$$\left\{ [d + \eta(t)]/d \right\} \int_0^d C_D \frac{W}{2g} D v_{rms} \sqrt{\frac{8}{\pi}} v dz = \\ = \left\{ [d + \eta(t)]/d \right\} \int_0^d C_D \frac{W}{2g} D v_{rms} \sqrt{\frac{8}{\pi}} \int_{-\infty}^{\infty} k_v(\tau; z) \eta(t-\tau) d\tau dz \\ = \left\{ [d + \eta(t)]/d \right\} \int_{-\infty}^{\infty} \left[C_D \frac{W}{2g} D v_{rms} \sqrt{\frac{8}{\pi}} \int_0^d k_v(\tau; z) dz \right] \eta(t-\tau) d\tau \quad (88)$$

Thus the quantity in the bracket is the kernel for the estimation of total force. The system function for the total drag force will be the Fourier

transform of the bracketed quantity or

$$K_{\text{total drag}}(f) = C_D \frac{w}{2g} D v_{\text{rms}} \sqrt{\frac{8}{\pi}} \int_0^d K_v(f; z) dz \quad (89)$$

Similarly from (66)

$$K_{\text{total inertial}}(f) = C_M \frac{w}{g} \frac{\pi D^2}{4} \int_0^d K_a(f; z) dz \quad (90)$$

and

$$K_{\text{total force}}(f) = K_{\text{total drag}}(f) + K_{\text{total inertial}}(f) \quad (91)$$

The system functions within (89) and (90) are given by (57) and (58). The integrations in (89) and (90) are easy to make and the result is

$$\begin{aligned} K_{\text{total force}}(f) = & C_D \frac{w}{2g} D v_{\text{rms}} \sqrt{\frac{8}{\pi}} \left(\frac{2\pi f}{k} \right) (\cos kh - i \sin kh) + \\ & + C_M \frac{w}{g} \frac{\pi D^2}{4} \frac{(2\pi f)^2}{k} (\sin kh - i \cos kh) \end{aligned} \quad (92)$$

This system function can be approximated with a Fourier series to obtain $\hat{K}_{\text{total force}}(f)$ and with it the digital filter which acts on the sea surface to simulate the total force on a single vertical pile.

The above development was based on a unidirectional wave spectrum and a linear approximation to drag force. The cubic approximation would lead to a third-order filter. The analysis would be parallel to the above but somewhat more complicated.

The complications can be avoided by a slightly different approach which involves, however, many more Fourier fits to determine digital filters. Suppose the digital filters for velocity and acceleration are computed at a series of

points up the pile between the sea floor and still water level.

Then the force at the k-th position is (using the cubic approximation),

$$f_k(m\Delta t) = \sum_{n=-N}^N a_{fn}^{(z)} \eta(m\Delta t - n\Delta t) + \sum_{n'=-N}^N \sum_{n''=-N}^N \sum_{n'''=-N}^N a_{f;n',n'',n'''}^{(z)} \eta(m\Delta t - n'\Delta t) \eta(m\Delta t - n''\Delta t) \eta(m\Delta t - n'''\Delta t) \quad (93)$$

with

$$a_{fn}^{(k)} = C_D \frac{w}{2g} D \sqrt{\frac{2}{\pi}} (v_{rms}) a_{vn}^{(k)} + C_M \frac{w}{g} \frac{\pi D^2}{4} a_{an}^{(k)} \quad (94)$$

$$a_{f;n',n'',n'''}^{(k)} = C_D \frac{w}{2g} D \sqrt{\frac{2}{9\pi}} \frac{a_{vn'}^{(k)} a_{vn''}^{(k)} a_{vn'''}^{(k)}}{v_{rms}} \quad (95)$$

and $a_{vn}^{(k)}$ and $a_{an}^{(k)}$ are the digital filter coefficients at the elevation for the k-th position on the pile. The total force may be computed by numerical integration of (93) to provide a cubic digital filter for total force.

$$F_{total}(m\Delta t) = \sum_{n=-N}^N a_{fn}^{(T)} \eta(m\Delta t - n\Delta t) + \sum_{n'=-N}^N \sum_{n''=-N}^N \sum_{n'''=-N}^N a_{f;n',n'',n'''}^{(T)} \eta(m\Delta t - n'\Delta t) \eta(m\Delta t - n''\Delta t) \eta(m\Delta t - n'''\Delta t) \quad (96)$$

with

$$a_{fn}^{(T)} = \sum_k a_{fn}^{(k)} \Delta z_k \quad (97)$$

$$a_{f;n',n'',n'''}^{(T)} = \sum_k a_{fn'}^{(k)} a_{fn''}^{(k)} a_{fn'''}^{(k)} \Delta z_k \quad (98)$$

where Δz_k is the appropriate vertical increment for the k-th position on the pile.

The total force can be "stretched" to correct for sea surface elevation variations by multiplying $F_{\text{total}}(m\Delta t)$ by $[\eta(m\Delta t) + d]/d$.

Total Force on a Group of Piles. - One procedure for simulating the total force on a group of vertical piles would be as follows. The sea surface elevations are first simulated for some central position within the group of piles. This is used as a common input for the digital filter simulation of the force on each of the piles. That is, each pile would have a different h value in (57), (58), and (92), which would be the x-direction spacing between the central position and the pile. If desired, the sea surface elevation at each pile could also be simulated from the sea surface elevations at the central position. All these together could then be used to determine the time series for total force. Of course, if the total force on each pile is not going to be corrected for sea surface elevations at that pile, the sea surface simulations can be dispensed with. In this case, the force digital filter coefficients for each pile can be added to give a single digital filter which acts on the sea surface elevations at the central position to provide as output the simulation for total force on the group of piles.

AN APPLICATION

Wave forces were measured near Davenport, California in 1953.¹⁶ The values of C_D and C_M were determined for a number of waves by the following procedure. The sea surface elevations were scanned and "well-defined" waves were selected. The wave force was read from the record at the crest and at the still water level crossing of each wave profile. The height and period for each wave was

used, with linear wave theory, to compute the water velocity and acceleration in the vicinity of the force sensing instrument at the crest and zero crossing phases of the wave. These theoretical velocities and accelerations were used with the measured forces to determine C_D and C_M . The procedure is considerably simplified by the theoretical relation that the inertial force is zero beneath the crest and the drag force is zero beneath the zero-crossing.

The values of C_D and C_M so computed showed a very large scatter. There are a number of possible reasons why this might happen. The forces might be inherently random so that C_D and C_M actually do vary. Vibrations or other recording difficulties may have introduced inaccuracies. Perhaps the irregularities in the wave profiles were sufficient to invalidate the theoretical computations. And there are other possibilities.

As a means of estimating the effect of profile irregularity on the C_D and C_M computations, a time history of sea surface elevation and water velocity and acceleration was simulated by the method of (7) and (62). The spectral density for the recorded waves on roll 10 of the Davenport data was used in the simulation. The agreement of the spectral density of the simulated sea surface and the Davenport spectral density is shown in Fig. 2. The velocities and accelerations were simulated at the same elevation above the sea floor as was used in the roll 10 measurements. The force at the instrument level was computed from the simulated velocities and accelerations using (64) and a C_D value of 1.0 and C_M of 2.0. Hence the simulations provided a sea surface time history and the force record which would result if the usual force formula, (64), were to hold exactly with the specified values of C_D and C_M .

Now the same analysis procedure used for the Davenport data was applied to this sea surface and force record. Well defined waves were selected from

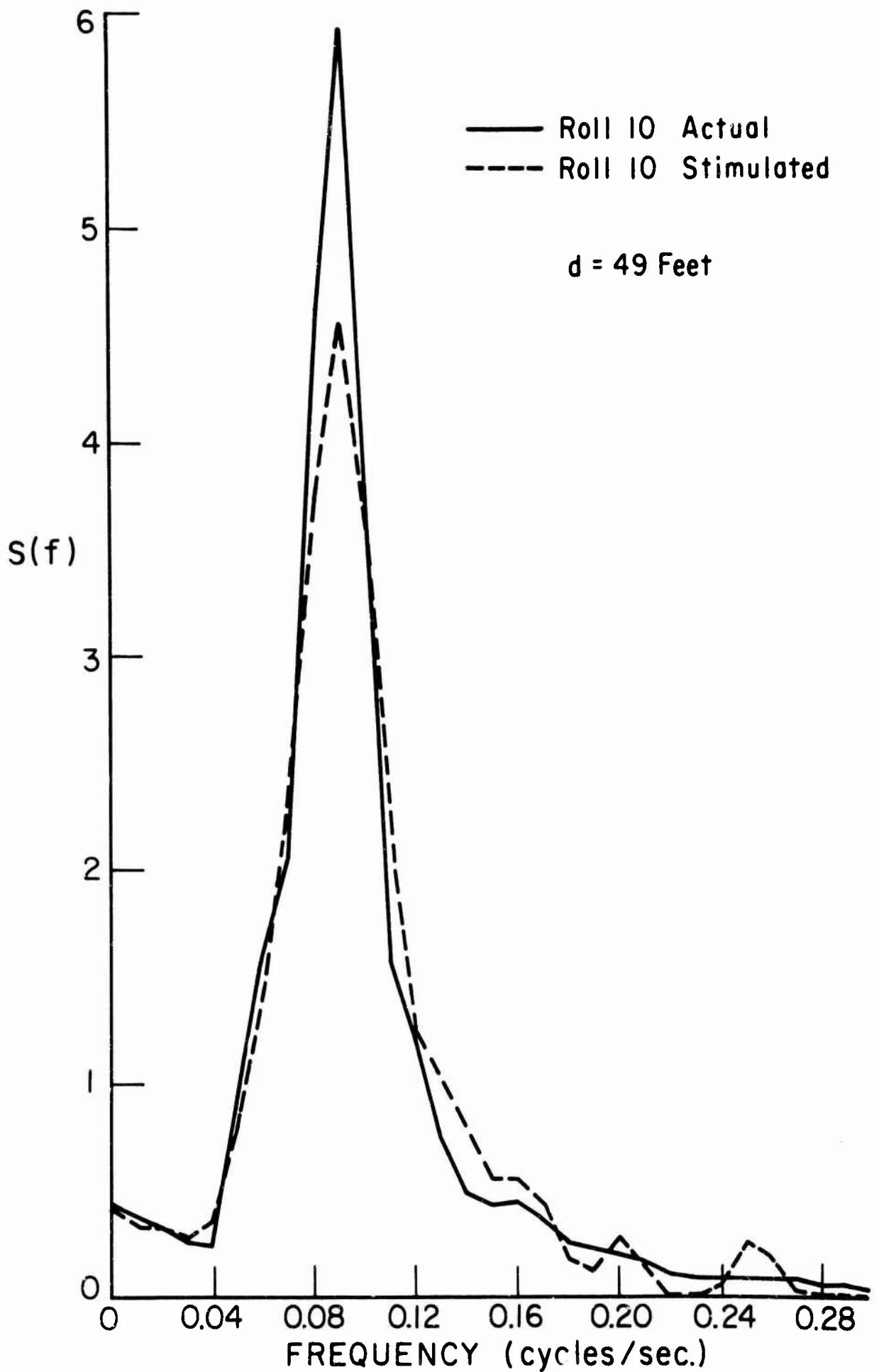


Fig. 2. Simulated and actual spectral densities for Davenport data, roll 10.

the sea surface elevations. The forces were read from the simulation beneath each wave crest and wave zero-crossing. Linear theory was used to compute the velocity beneath the crest and the acceleration beneath the profile zero-crossing. These values were combined to estimate C_D and C_M . If the method were accurate, $C_D = 1.0$ and $C_M = 2.0$ would be the result.

The scatter diagram for the computed C_D and C_M values is shown in Fig.3. There is considerable scatter. Fig. 4 provides a plot of C_D versus Reynolds number and Fig. 5 gives a ranked plot of C_M on normal probability paper. The figures are strikingly similar to the corresponding results for the Davenport data and suggests that the wave profile irregularities contributed considerably to the C_D and C_M scatter in the Davenport results.

CONCLUSIONS

1. Techniques for simulating ocean waves are most applicable when the response of the structure is complicated and perhaps involves other random environmental factors that may be introduced by concurrent simulations.
2. The accuracy of the wave simulation is greatest for low amplitude waves and decreases for large steep waves. The degree of loss in accuracy for the higher and steeper waves deserves further research.
3. Simulation techniques have the disadvantage of being time consuming and usually requiring the use of computers. Analytic solutions are to be preferred if feasible. Sometimes part of a problem can be solved analytically and then the intractable parts processed by simulation. A detailed search for shortcuts and approximations before proceeding with the actual simulation will often result in sizeable savings of computer time.
4. The engineer will usually be forced to simulate with one-dimensional spectral densities because there are so few reliably measured two-dimensional

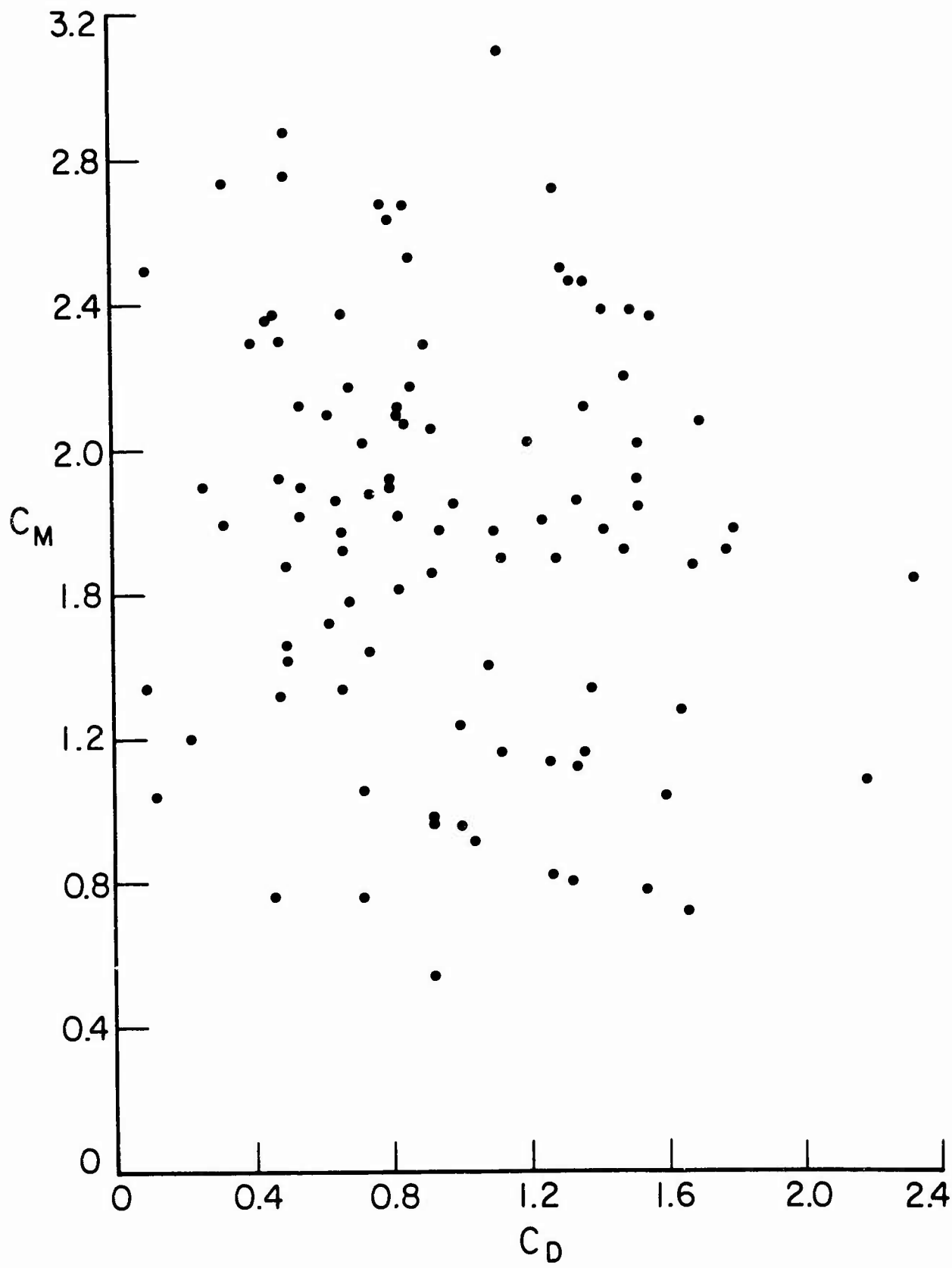


Fig. 3. C_D and C_M values computed from the simulations.

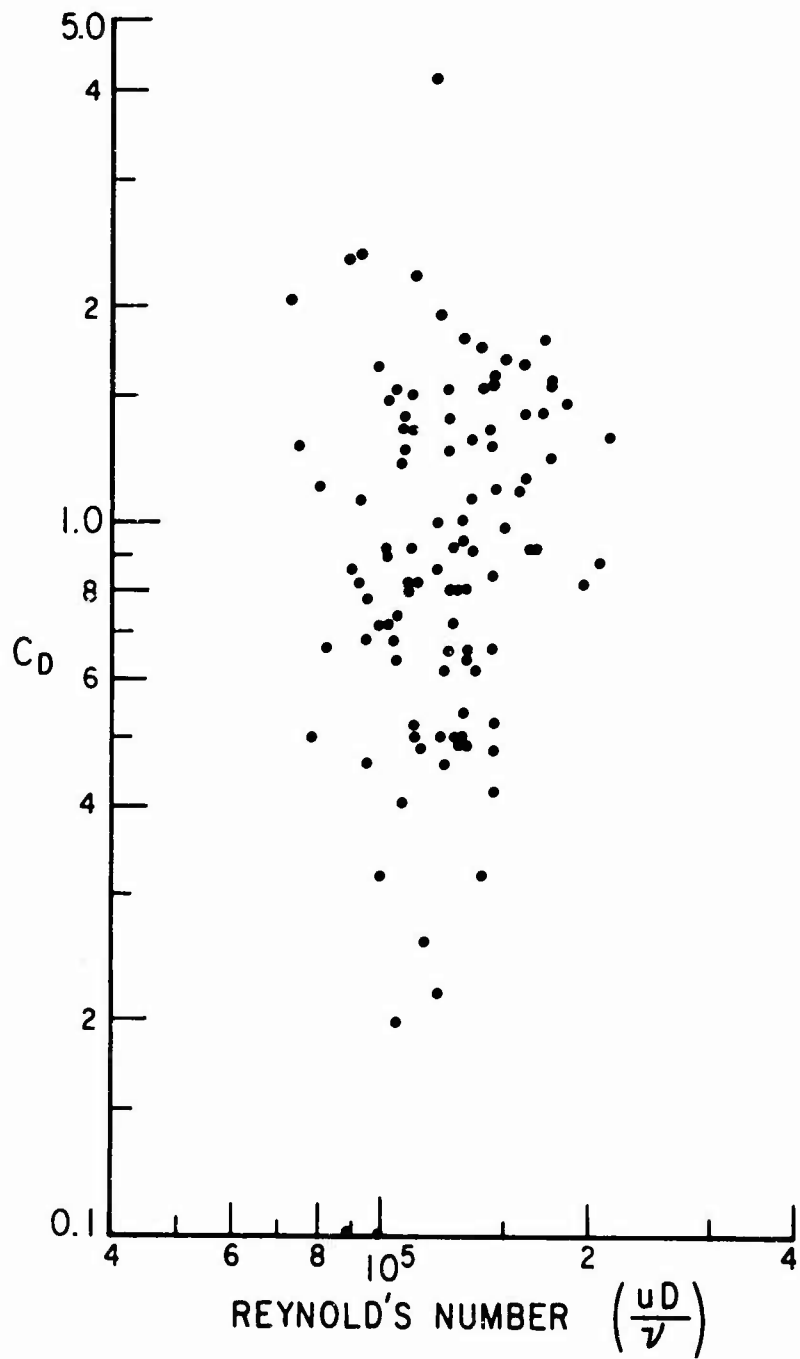


Fig. 4. C_D values from the simulations plotted versus Reynold's number.

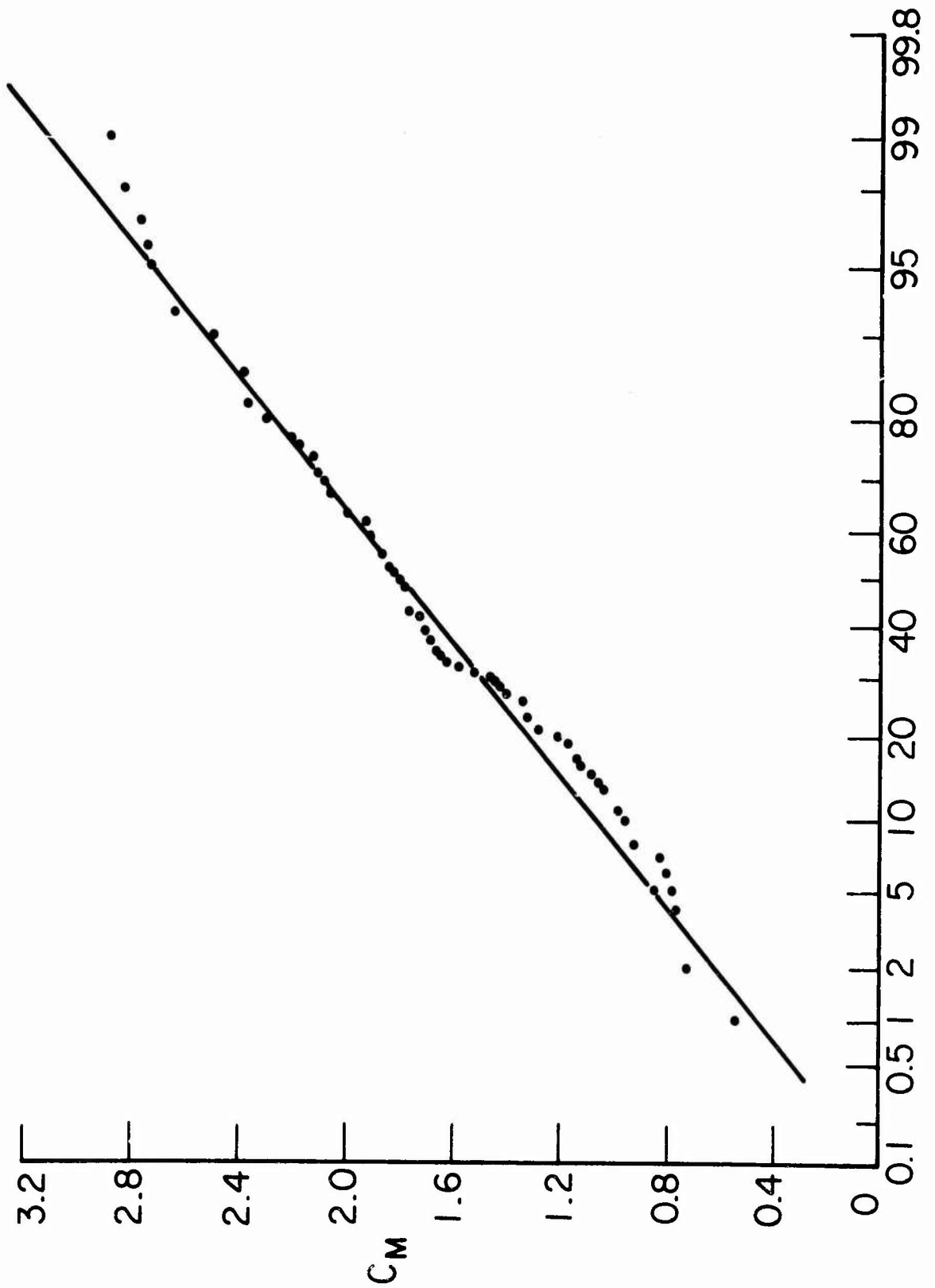


Fig. 5. C_M from simulations plotted on normal paper.

spectral densities. The formulas for 2-D spectra were included in the hope that satisfactory directional data will soon be available.

5. The linearization of the drag force, or its approximation by polynomials, is particularly useful in many problems. However, in some applications, it is just as easy to work with the $v|v|$ term directly.

ACKNOWLEDGMENTS

The writer wishes to express his appreciation to the Coastal Engineering Research Center, Corps of Engineers, U. S. Department of the Army, for their support of this work under contract DA-49-055-CIV-ENG-64-6. In addition, the writer would like to thank Dr. L. J. Brown and Mr. K. W. Gay for their assistance in various aspects of the study.

APPENDIX I. - FOURIER TRANSFORM OF A WEIGHTED DIRAC COMB

$$\begin{aligned}
 \hat{K}(f) &= \int_{-\infty}^{\infty} e^{-i2\pi f\tau} \sum_{n=-N}^N a_n \delta(\tau - n\Delta t) d\tau \\
 &= \sum_{n=-N}^N a_n e^{-i2\pi fn\Delta t} \\
 &= \sum_{n=-N}^N \left[\frac{1}{2} (a_n + a_{-n}) + \frac{1}{2} (a_n - a_{-n}) \right] e^{-in\pi f(2\Delta t)} \\
 &= \sum_{n=-N}^N [A_n + B_n] e^{-in\pi f/F} \tag{99}
 \end{aligned}$$

where

$$A_n = \frac{1}{2} (a_n + a_{-n}) \quad (100)$$

$$B_n = \frac{1}{2} (a_n - a_{-n}) \quad (101)$$

$$F = 1/2 \Delta t \quad (102)$$

This definition results in the symmetries

$$A_n = A_{-n} \quad (103)$$

$$B_n = -B_{-n} \quad (104)$$

Hence

$$\begin{aligned} \hat{K}(f) &= A_0 + \sum_{n=1}^N A_n (e^{-in\pi f/F} + e^{in\pi f/F}) \\ &\quad + \sum_{n=1}^N B_n (e^{-in\pi f/F} - e^{in\pi f/F}) \\ &= A_0 + 2 \sum_{n=1}^N A_n (e^{in\pi f/F} + e^{-in\pi f/F})/2 \\ &\quad - 2i \sum_{n=1}^N B_n (e^{in\pi f/F} - e^{-in\pi f/F})/2i \end{aligned} \quad (105)$$

Since

$$\cos \theta = (e^{i\theta} + e^{-i\theta})/2 \quad (106)$$

$$\sin \theta = (e^{i\theta} - e^{-i\theta})/2i \quad (107)$$

The previous equation reduces to

$$\hat{K}(f) = A_0 + 2 \sum_{n=1}^N A_n \cos(n\pi f/F) - 2i \sum_{n=1}^N B_n \sin(n\pi f/F) \quad (108)$$

APPENDIX II. - INPUT-OUTPUT RELATIONS FOR MULTIPLE SIMULATIONS

Using the notation of eq. (42) and following

$$y_m(t) = \sum_{j=1}^m \int_{-\infty}^{\infty} k_{mj}(y) x_j(t-y) dy \quad (109)$$

Let $m \geq r$. Then

$$\begin{aligned} C_{mr}(\tau) &= E[y_m(t) y_r(t+\tau)] \\ &= E\left[\sum_{j=1}^m \int_{-\infty}^{\infty} k_{mj}(y) x_j(t-y) dy \sum_{j'=1}^r \int_{-\infty}^{\infty} k_{rj'}(z) x_{j'}(t+\tau-z) dz \right] \\ &= \sum_{j=1}^m \sum_{j'=1}^r \int_{-\infty}^{\infty} \int_{-\infty}^{\infty} k_{mj}(y) k_{rj'}(z) E[x_j(t-y) x_{j'}(t+\tau-z)] dy dz \\ &= \sum_{j=1}^r \int_{-\infty}^{\infty} \int_{-\infty}^{\infty} k_{mj}(y) k_{rj}(z) C_{x_j x_j}(\tau-z+y) dy dz \quad (110) \end{aligned}$$

One summation is eliminated by the independence of the inputs. The summand is zero unless $j = j'$. By definition

$$s_{x_j x_j}(f) = \int_{-\infty}^{\infty} e^{-i2\pi f\tau} C_{x_j x_j}(\tau) d\tau \quad (111)$$

and

$$C_{x_j x_j}(\tau) = \int_{-\infty}^{\infty} e^{i2\pi f\tau} s_{x_j x_j}(f) df \quad (112)$$

If (112) is substituted into (110) and it is assumed the functions involved permit interchange of integration order, then

$$\begin{aligned}
C_{mr}(\tau) &= \sum_{j=1}^r \int_{-\infty}^{\infty} \int_{-\infty}^{\infty} k_{mj}(y) k_{rj}(z) \int_{-\infty}^{\infty} e^{i2\pi f(\tau - z + y)} s_{x_j x_j}(f) df dy dz \\
&= \sum_{j=1}^r \int_{-\infty}^{\infty} \left[\int_{-\infty}^{\infty} k_{mj}(y) e^{i2\pi f y} dy \int_{-\infty}^{\infty} e^{-i2\pi f z} k_{rj}(z) dz s_{x_j x_j}(f) \right] e^{i2\pi f \tau} df \\
&= \int_{-\infty}^{\infty} \left[\sum_{j=1}^r \overline{K_{mj}(f)} K_{rj}(f) s_{x_j x_j}(f) \right] e^{i2\pi f \tau} df \tag{113}
\end{aligned}$$

(The over bar indicates complex conjugation.)

Again, by definition of $C_{mr}(\tau)$, analogously to (112)

$$C_{mr}(\tau) = \int_{-\infty}^{\infty} s_{mr}(f) e^{-i2\pi f \tau} df \tag{114}$$

If (114) is compared with (113), it can be seen that

$$s_{mr}(f) = \sum_{j=1}^r K_{mj}(f) \overline{K_{rj}(f)} s_{x_j x_j}(f) \tag{115}$$

If the inputs are white noise, the input spectral densities are unity and

$$s_{mr}(f) = \sum_{j=1}^r K_{mj}(f) \overline{K_{rj}(f)} \tag{116}$$

Since

$$s_{mr}(f) = \overline{s_{rm}(f)} \tag{117}$$

(116) determines $s_{mr}(f)$ for all m and r between 1 and M .

APPENDIX III. - NOTATION

The following symbols are used in this paper:

- a = horizontal component of acceleration;
- a_n = weighting coefficient in a digital filter (see eq.(17));
- a^2 = increment in $S(f)$ (see eq.(7) ff.);
- A = a constant in the Bretschneider-Pierson spectral density formula
(see eq.(10));
- A_n = coefficients in Fourier transform of a digital filter (see eq.(30));
- B = a constant in the Bretschneider-Pierson spectral density formula
(see eq.(10));
- B_n = coefficients in Fourier transform of a digital filter;
- c = coefficient in optimal linear approximation of drag force
(see eq.(72));
- c_n = coefficients in optimal polynomial fitting to drag force;
- C_D = drag coefficient;
- C_M = inertial coefficient;
- d = water depth;
- D = pile diameter;
- f = frequency in cycles per unit time
- \hat{f}_n = midpoint of the n-th increment of frequency (see eq.(2));
- F = cutoff frequency - the highest frequency important in the response
or a frequency such that $s(f) \approx 0$ for $f > F$;
- g = gravity;
- h = space lag in x direction (see eq.(55));
- $\Im[z]$ = imaginary part of z;

k = wave number;
 $k(\tau)$ = kernel in a linear operator (see eq.(18));
 \hat{k} = wave number in radians per unit length corresponding to frequency \hat{f} (see eq.(4));
 $K(f)$ = Fourier transform of $k(\tau)$, $K(f)$ is called the system function;
 m = mean velocity in eq.(83);
 N = number of increments in simulation by superposition;
 Q = quantity to be minimized in least-square fitting (see eq.(72));
 Q_n = coefficients in the normal-to-gamma transformation (see eq.(50));
 $\Re [z]$ = real part of z ;
 s_k = skewness;
 $s(f)$ = spectral density;
 $s_{xx}(f)$ = spectral density of $x(t)$;
 $s_{xy}(f)$ = cross-spectral density of $x(t)$ and $y(t)$;
 $s_{mr}(f)$ = cross-spectral density between $y_m(t)$ and $y_r(t)$ in the development following eq.(42);
 $S(f)$ = Cumulative spectrum (see eq.(6));
 t = time;
 v = horizontal component of velocity;
 v_{rms} = root-mean-square velocity, or standard deviation of the velocity;
 w = specific weight of water;
 x = one of the horizontal coordinates;
 x = v/v_{rms} (see eq.(79) ff.);
 x = variate in standard normal formulas (eqs.(84) and (85));
 $x(t)$ = general input for linear operators;
 x_n = n-th element in input sequence for a digital filter (see eq.(17));

- X_n = coefficients in the gamma-to-normal transformation (eq.(52));
 y = one of the horizontal coordinates;
 y_k = k-th element in the output sequence of a digital filter
 (see eq.(17));
 z = coordinate measured vertically upward from sea floor;
 $\delta(t)$ = Dirac delta function;
 Δf_n = n-th increment of frequency (see eq.(1));
 Δt = time increment in application of a digital filter;
 $\Delta \theta_m$ = m-th increment of θ ;
 $\eta(t)$ = sea surface elevation above still water level;
 $\hat{\eta}_s(t)$ = skewed version of $\hat{\eta}(t)$;
 $\hat{\eta}(t)$ = simulated sea surface elevation above still water level at time t ;
 θ = direction variable in a directional spectrum;
 θ = wave phase angle in eqs.(70) and (71);
 $\hat{\theta}_m$ = midpoint of the m-th increment of θ ;
 σ = standard deviation of velocity = v_{rms} ;
 ϕ = wave force;
 $\phi(x)$ = standard normal probability density (eq.(84));
 Φ = random phase; and
 $\Phi(x)$ = distribution function for a standard normal variate (eq.(85)).